Support Information

Li-Na Wu, [a] Jun Peng, [a] Fa-Ming Han, [a] Ya-Ke Sun,[a] Tian Sheng, [c] Yang-Yang Li,[a]

Yao-Zhou, [b] Ling Huang, *[a] Jun-tao Li, [b] and Shi-Gang Sun *[a,b]

[a] *Department of Chemistry, College of Chemistry and Chemical Engineering, Xiamen University, Xiamen, Fujian, 361005, China*

[b] *College of Energy and School of Energy Research, Xiamen University, Xiamen, Fujian 361005, China*

c College of Chemistry and Materials Science, Anhui Normal University, Wuhu, Anhui 241000,China

* *Corresponding author*

E-mail: huangl@xmu.edu.cn

E-mail: sgsun@xmu.edu.cn

Experimental Section

Li metal foil (Shenzhen Kejingstar, 0.4 mm) was used as the anode electrode. The graphite positive electrode was prepared by mixing of graphite, conductive carbon black, and poly-vinylidene fluoride (PVDF) in N-methyl-2-pyrrolidone (NMP) with a weight ratio of 8:1:1. The above mixture was stirring constantly to form uniform slurry at room temperature, which was then coated onto aluminum current collector (Shenzhen Kejingstar) and dried in vacuum in an 80 °C oven. The active materials loading in graphite cathode are 2.0~2.5 mg cm^{-2}.

A glass microfiber filter (Whatman, grade 934-AH) was used as the separator. Lithium hexafluorophosphate ($LiPF_6$), ethyl methyl carbonate (EMC) and vinylene carbonate (VC) were purchased from Dodochem. The $AgPF_6$ and $LiNO_3$ additive were kindly purchased from Alfa Aesar. The base electrolyte was composed of 4M $LiPF_6$, EMC and VC (the 3vol% VC additive can improve the uniformity and flexibility of the interface film on electrode materials surface [1-3]). The 0.03 M $LiNO_3$ and $AgPF_6$ additive were added as important additives to improve the electrochemical performance of Li electrode. The effect of $LiNO_3$ was discussed in the reported work. The solubility of additives in the base electrolyte in 15^{th} day at 30℃ is shown in the optical image (Fig.S1). The preparation of electrolyte and fabrication of CR2025-type coin cells were conducted in an argon-filled glove box (MBraun, Germany) with the oxygen and water level below 0.1 ppm. When assembling a symmetric cell, Li electrodes were both employed on both sides of the separator. The electrolyte was composed of base electrolyte with or without additive. And for the Li-Graphite Dual-ion cells, Li electrode was used as anode, and graphite electrode was used as cathode. The electrolyte was also composed of base electrolyte with or without $AgPF_6$-$LiNO_3$ hybrid electrolyte additive. And then the electrochemical performance was performed on a battery test system (LAND CT2011A).

Characterization and Electrochemical tests

X-ray photoelectron spectroscopy (XPS) was carried out using Thermo Fisher Scientific K-Alpha. Scanning electron microscope (SEM) images were collected on a HITACHI S-4800 field emission scanning electron microscope (operating at 10 kV). The linear sweep voltammogram (LSV) curves of Li^+ deposition on the Li anode were obtained in a three-electrode cell using the Li metal electrodes as the working electrode, counter electrode and reference electrode with a CHI660D electrochemical station (Chenhua, China) at a scan rate of 1mV s^{-1}. The area of the working electrode was 2.51 cm^2. Galvanostatic charge–discharge tests were worked on LAND CT2011A battery testing instrument at room temperature. The electrochemical impedance spectrum (EIS) experiment test was carried out on a CHI760e electrochemical station (Chenhua, China). The ac voltage amplitude was 5 mV and the range of frequency was from 100 kHz to 10 mHz.

Computational methods

Density functional theory (DFT) calculations were carried out using the Vienna Ab initio Simulation Package (VASP) program. Generalized gradient approximation (GGA) functional Perdew–Burke–Ernzerhof (PBE) functional of exchange-correlation and the projector-augmented-wave pseudopotentials were here utilized [4-8].

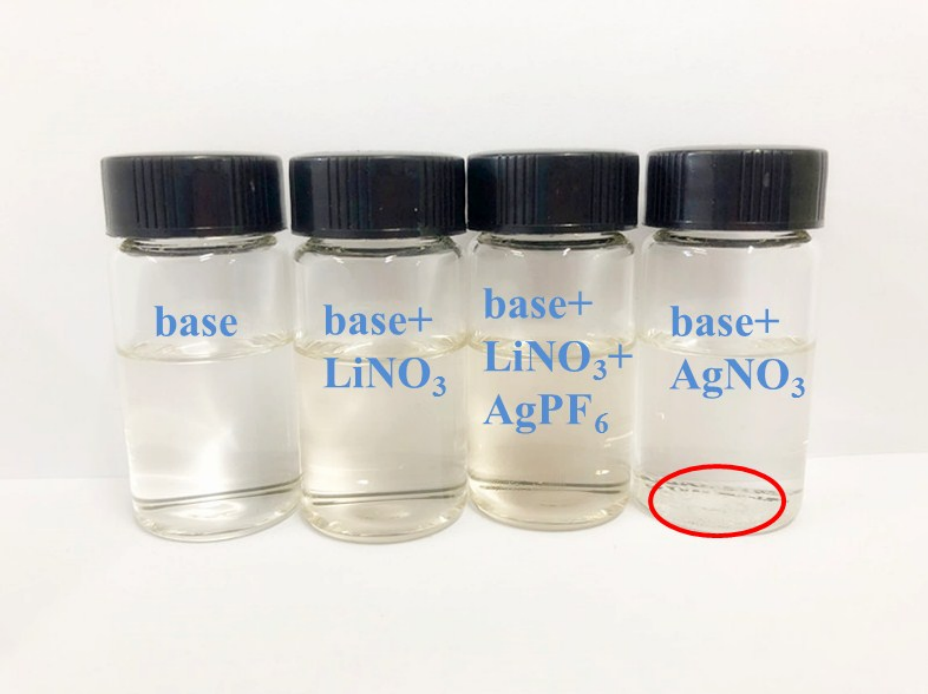

Fig.S1 The solubility of additives in the base electrolyte in 15th day at 30℃

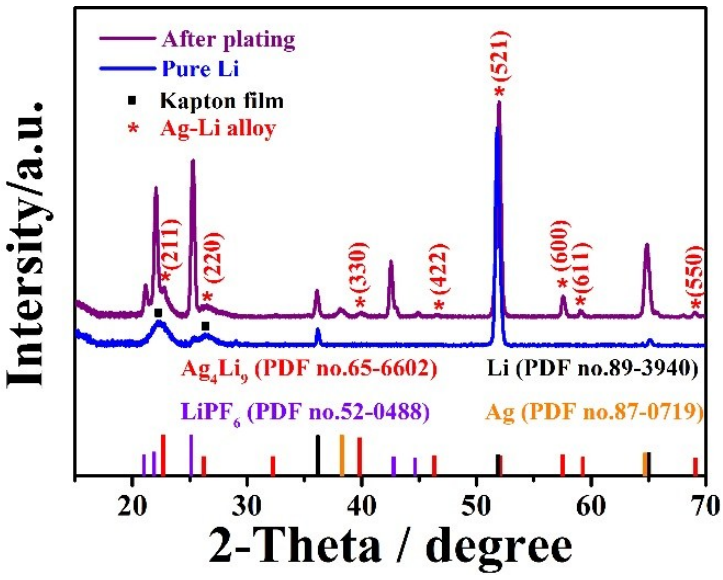

Fig.S2 XRD pattern of the pure Li foil and the Li foil after plating

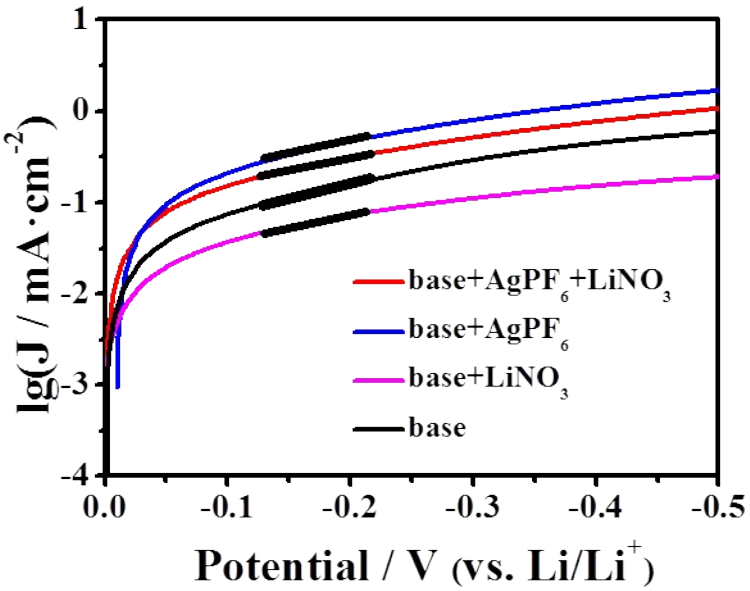

Figure S3 Exchange current densities of Li anodes in base electrolyte with different additive at 25℃ as determined by fitting LSV curves.

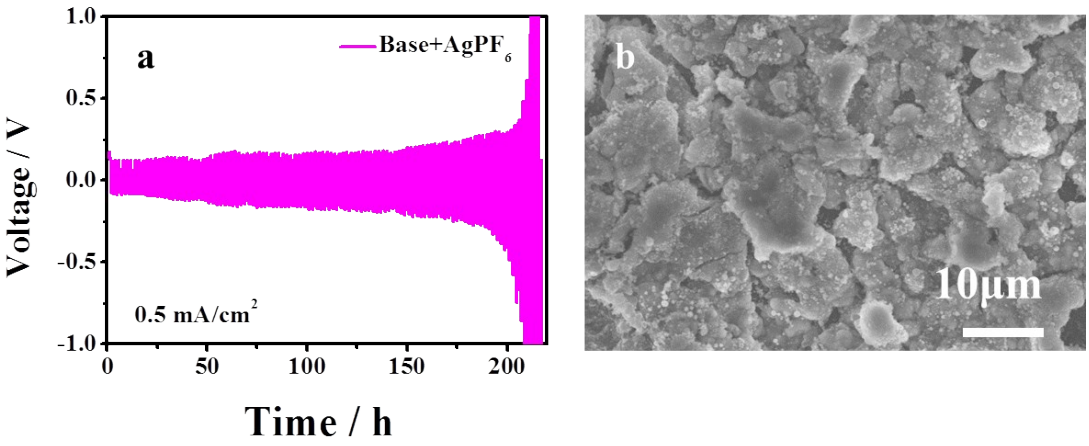

Figure S4 (a) The cycling performance of Li||Li symmetric cells with only $AgPF_6$ additive at current densities of 0.5 mA cm^{-2}.
(b) SEM images of Li anode after plating and stripping for 200 h in the base electrolyte with only $AgPF_6$ additives.

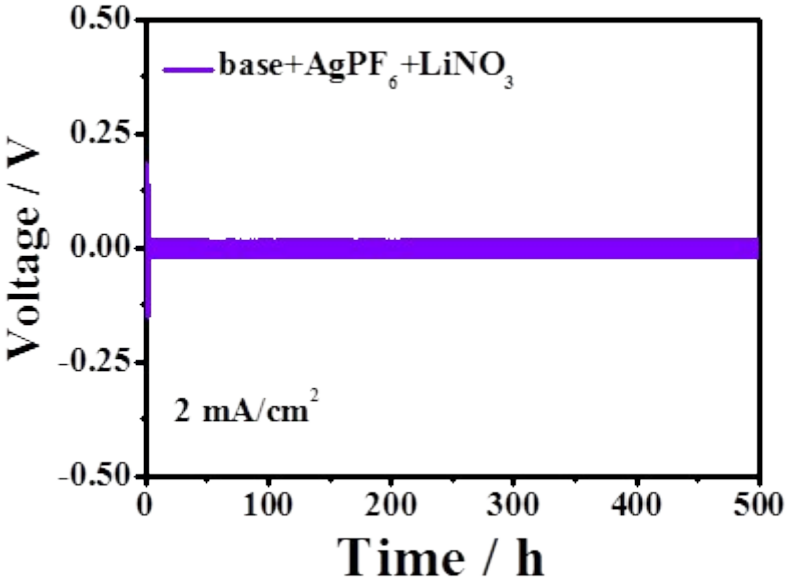

Figure S5 Cycling performance of Li||Li symmetric cells with $AgPF_6$-$LiNO_3$ additive at current densities of 2.0 mA cm^{-2}.

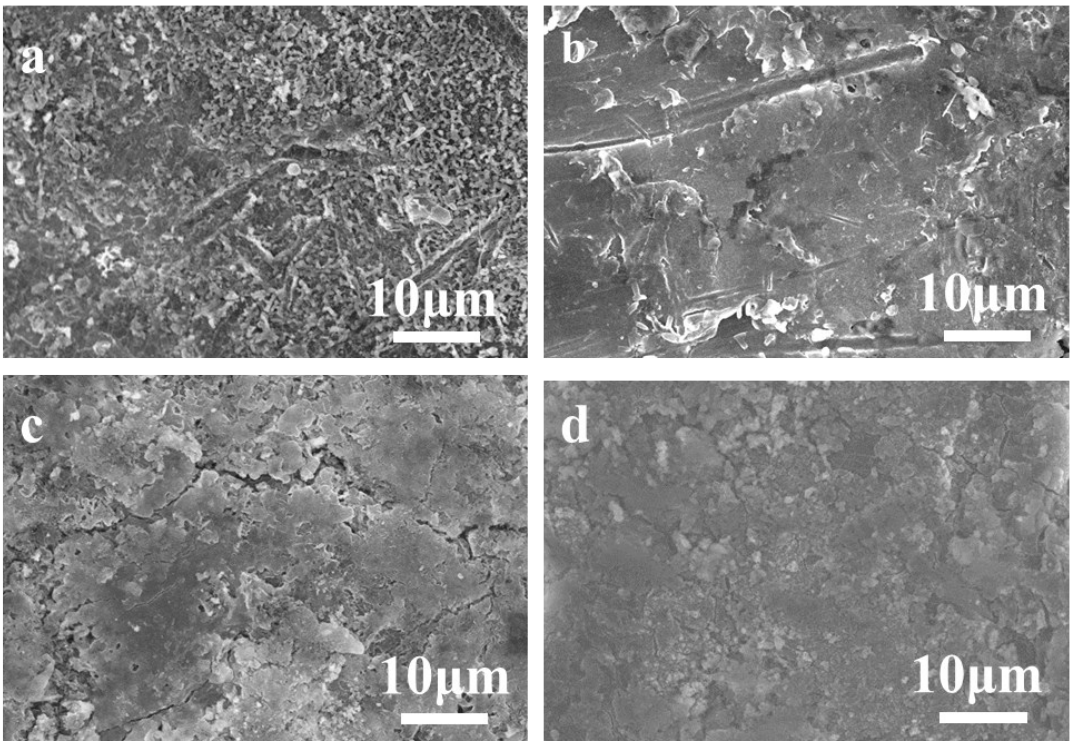

Figure S6 SEM images of Li anode after plating and stripping for 40 h in the baseline electrolyte (a) and in the base electrolyte with $LiNO_3$ additive (b). The SEM images of Li anode after plating and stripping for 200 h in the base electrolyte with $LiNO_3$ additive (c) and with $AgPF_6$-$LiNO_3$ additive (d).

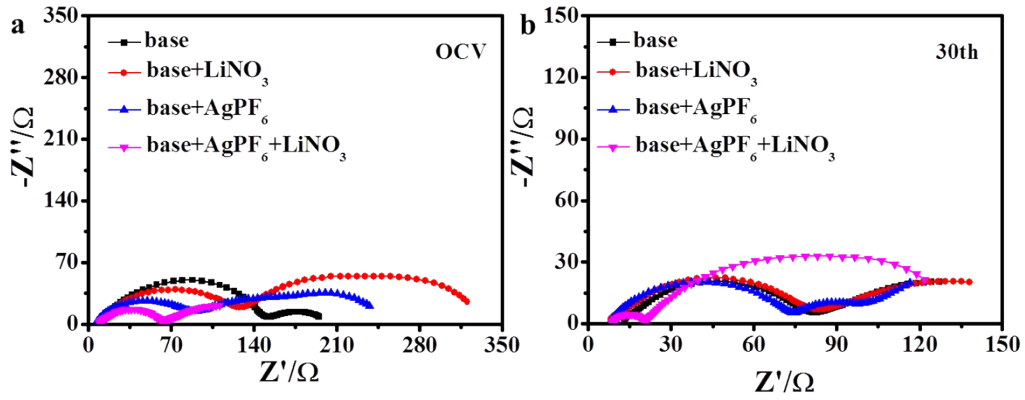

Figure S7 EIS of the Li||Li symmetric cell before cycling (a) and after 30 cycles (b) at a current density of 0.5 mA cm^{-2} without or with different additives.

Table S1 The fitted value of electrochemical impedance spectroscopy (EIS) about the Li||Li symmetric cell before cycling (a) and after 30 cycles (b) at a current density of 0.5 mA cm^{-2} with fixed capacity of 0.5 mAh cm^{-2} without or with different additives.

	R_{SEI} (OCV)	$R_{SEI}(30^{th})$
base	38.82	61.73
base+$LiNO_3$	118.5	64.24
base+$AgPF_6$	79.65	66.9
base+ $AgPF_6$+ $LiNO_3$	43.93	12

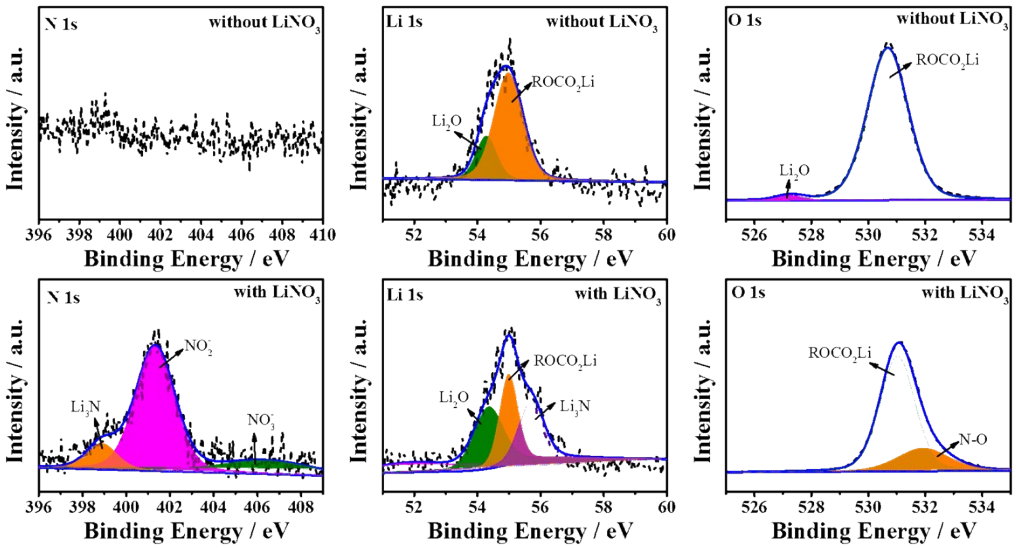

Fig. S8 XPS characterization for the Li anode cycled in electrolyte without and with $LiNO_3$.

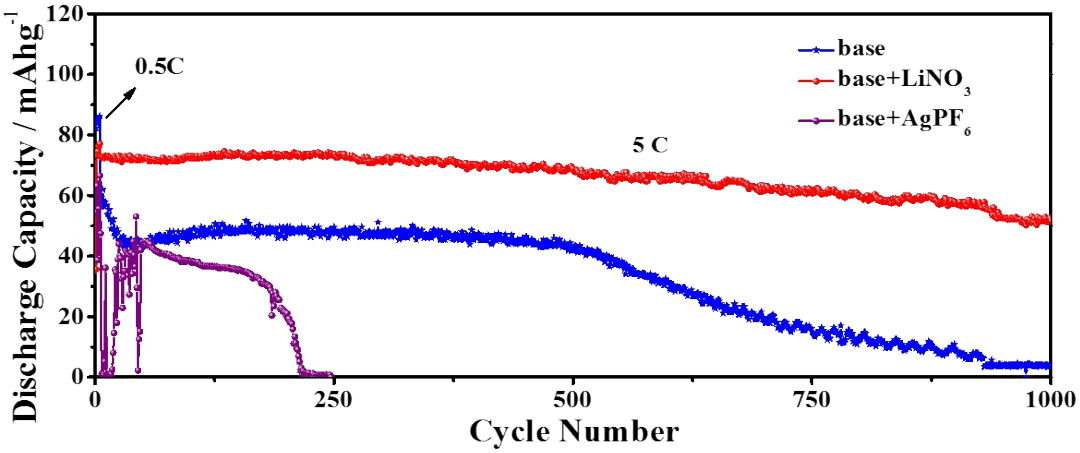

Figure S9 Long-term test results of the Li-G DIB without or with $LiNO_3$ additive or with $AgPF_6$ additive at 0.5 C (1 to 10 cycles) and 5C (11 to 1000 cycles).

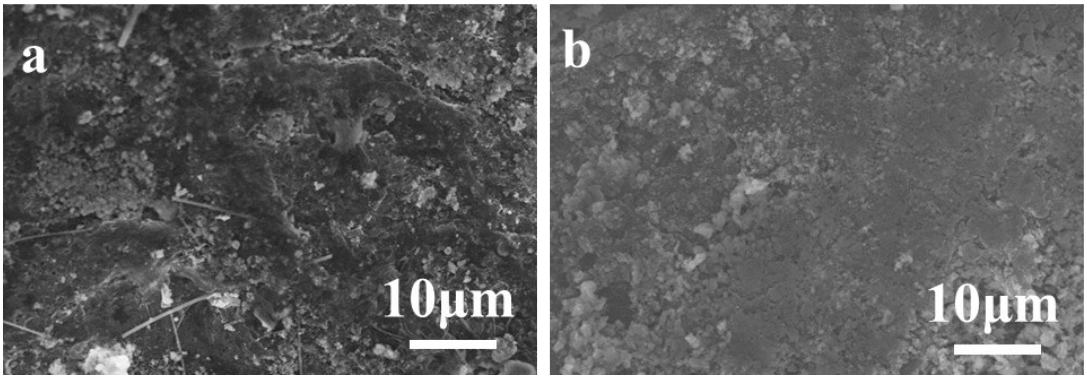

Figure S10 SEM images of the Li anode in electrolyte with $LiNO_3$ additive (a) or with $AgPF_6$ - $LiNO_3$ additive (b) after 500 cycles at 5 C.

Table S2. Performance comparison of this work and reported DIBs.

DIB structure	Reversible capacity	Capacity retention	Cycle number	Estimated energy density	Reference
CNFs-Li|$LiPF_6$ -EMC |Graphite	92.2 mAh g^{-1} (1000 mA g^{-1})	86.4%	2000	———	[9]
Graphite|$LiPF_6$-FEC EMC-HFIP|Graphite	60 mAh g^{-1} (50 mA g^{-1})	67%	50	———	[10]
Si-compound|$LiBF_4$ -PC|Graphite	80 mAh g^{-1} (100 mA g^{-1})	84%	100	54 Wh kg^{-1}	[11]
MoO_3|$LiPF_6$-EC-DMC| Graphite	81 mAh g^{-1} (100 mA g^{-1})	90%	200	77 Wh kg^{-1}	[12]
TiO_2|$LiPF_6$-EC -DMC|Graphite	44 mAh g^{-1} (100 mA g^{-1})	88%	50	36 Wh kg^{-1}	[13]
Al|$LiPF_6$-EMC| Graphite	100 mAh g^{-1} (200 mA g^{-1})	88%	200	220 Wh kg^{-1} (130 W kg^{-1}); 150 Wh kg^{-1} (1200 W kg^{-1})	[14]
pAl/C|$LiPF_6$-EMC| Graphite	104 mAh g^{-1} (200 mA g^{-1})	89.4%	1000	232 Wh kg-1 (446 W kg-1); 180 Wh kg-1 (3597 W kg-1)	[15]
Li|LiTFSI-Pyr_{14}FTFSI| KS6L	50.1 mAh g^{-1} (50 mA g^{-1})	97%	500	100 Wh kg^{-1}	[16]
Li|$LiPF_6$-EMC | Graphite	69 mAh g^{-1} (400 mA g^{-1})	81%	1000	243 Wh kg^{-1} (486 W kg^{-1}); 350 Wh kg^{-1} (1750 W kg^{-1})	[17]
Li|$LiPF_6$-EMC -$AgPF_6$-$LiNO_3$| Graphite	80 mAh g^{-1} (500 mA g^{-1})	88%	1000	374 Wh kg^{-1} (748 W kg^{-1}); 360 Wh kg^{-1} (2250 W kg^{-1})	This work

Calculation method of specific energy density (see reference [14])

References

[1] L. Chen, K. Wang, X. Xie, and J. Xie, Effect of vinylene carbonate (VC) as electrolyte additive on electrochemical performance of Si film anode for lithium ion batteries, J. Power Sources. 174 (2007) 538-543.

[2] J. Chai, Z. Liu, J. Ma, J. Wang, X. Liu, H. Liu, J. Zhang, G. Cui, and L. Chen, In Situ Generation of Poly (Vinylene Carbonate) Based Solid Electrolyte with Interfacial Stability for LiCoO2 Lithium Batteries, Adv Sci (Weinh) 4 (2017) 1600377.

[3] P. Jankowski, W. Wieczorek, and P. Johansson, SEI-forming electrolyte additives for lithium-ion batteries: development and benchmarking of computational approaches, J Mol Model 23 (2017) 6.

[4] G. Kresse, and J. Hafner, Ab initio molecular dynamics for open-shell transition metals, Phys Rev B Condens Matter 48 (1993) 13115-13118.

[5] G. Kresse, and J. Furthmuler, Efficient iterative schemes for ab initio total-energy calculations using a plane-wave basis set, Phys. Rev. B 54 (1996) 11169-11186.

[6] J. P. Pedrew, K. Burke, and M. Ernzerhof, Generalized gradient approximation made simple, Phys. Rev. Lett. 77 (1996) 3865-3868.

[7] G. Kresse, and D. Joubert, From Ultrasoft pseudopotentials to the projector augmented-wave method., Phys. Rev. B 59 (1999) 1758-1775.

[8] P. E. Blochl, Projector augmented-wave method, Phys Rev B Condens Matter 50 (1994) 17953-17979.

[9] X. T. Xi, X. Feng, X. J. Nie, B. H. Hou, W. H. Li, X. Yang, A. B. Yang, W. D. Sun, and X. L. Wu, Dendrite-free deposition on lithium anode toward long-life and high-stable Li//graphite dual-ion battery, Chem. Commun. 55 (2019) 8406-8409.

[10] J. A. Read, A. V. Cresce, M. H. Ervin, and K. Xu, Dual-Graphite Chemistry Enabled by a High Voltage Electrolyte, Energy Environ. Sci. 7 (2014) 617-620.

[11] H. Nakano, Y. Sugiyama, Tetsuya Morishita, M. J. S. Spencer, I. K. Snook, Y. Kumaia, and H. Okamoto, Anion secondary batteries utilizing a reversible BF4 insertion/extraction two-dimensional Si material, Journal of Materials Chemistry A (2014) 7588-7592

[12] N. Gunawardhana, G.-J. Park, N. Dimov, A. K. Thapa, H. Nakamura, H. Wang, T. Ishihara, and M. Yoshio, Constructing a novel and safer energy storing system using a graphite cathode and a MoO3 anode, J. Power Sources. (2011)

[13] A. K. Thapa, G. Park, H. Nakamura, T. Ishihara, N. Moriyama, T. Kawamura, H. Wang, and M. Yoshio, Novel graphite/TiO2 electrochemical cells as a safe electric energy storage system, Electrochim. Acta 55 (2010) 7305-7309.

[14] X. Zhang, Y. Tang, F. Zhang, and C.-S. Lee, A Novel Aluminum-Graphite Dual-Ion Battery, Adv. Energy Mater. 6 (2016)

[15] L. N. Wu, J. Peng, Y. K. Sun, F. M. Han, Y. F. Wen, C. G. Shi, J. J. Fan, L. Huang, J. T. Li, and S. G. Sun, High-Energy Density Li metal Dual-Ion Battery with a Lithium Nitrate-Modified Carbonate-Based Electrolyte, ACS Appl. Mater. Inter. 11 (2019) 18504-18510.

[16] T. Placke, O. Fromm, S. F. Lux, P. Bieker, S. Rothermel, H. W. Meyer, S. Passerini, and M. Winter, Reversible Intercalation of Bis(trifluoromethanesulfonyl)imide Anions from an Ionic Liquid Electrolyte into Graphite for High Performance Dual-Ion Cells, J. Electrochem. Soc. 159 (2012) A1755-A1765.

[17] X. Tong, F. Zhang, B. Ji, M. Sheng, and Y. Tang, Carbon-Coated Porous Aluminum Foil Anode

for High-Rate, Long-Term Cycling Stability, and High Energy Density Dual-Ion Batteries, Adv. Mater. 28 (2016) 9979-9985.